

Closer look into the structures of tetrabutylammonium bromide–glycerol-based deep eutectic solvents and their mixtures with water

Patrycja Makoś-Chełstowska ^{a*}, Renáta Chromá ^b, Vasil Andruch ^b

^a Department of Process Engineering and Chemical Technology, Faculty of Chemistry, Gdansk University of Technology, Gdansk, PL-80-233 Gdańsk, Poland

^b Department of Analytical Chemistry, Institute of Chemistry, Faculty of Science, Pavol Jozef Šafárik University in Košice, SK-04154 Košice, Slovakia

*Corresponding author: dr Patrycja Makoś-Chełstowska, PhD. Eng.,
e-mail: patrycja.makos@pg.edu.pl

Abstract: In recent years, deep eutectic solvents (DES) and its mixture with water have become more and more attention as green solvents used in chemistry. However, there are only a few theoretical studies on the mechanisms of pure DES and DES-water complex formation. Therefore, the structural properties of tetrabutylammonium bromide–glycerol-based deep eutectic solvents and their mixtures with water have been investigated by means of Molecular Dynamics simulations. The obtained results indicate that three types of H-bonds exist in the pure DES structures, and all of these interactions play an important role in DES formation. In addition, between hydrogen bond donors (HBDs) and hydrogen bond acceptor (HBA) weaker non-bonded interactions, i.e. van der Waals exist, which also contribute to the formation of stable DES structures and to lower the melting point of DES compared to pure substances. The small addition of water to DES provides the formation of a stable complex, however, a further increase in water content (higher than 50% v/v) provide to the destruction of the most important hydrogen bonds (O–H···Br) in DES structure.

Keywords: Deep eutectic solvents, Tetrabutylammonium bromide, Glycerol, Theoretical calculations

35 **Abbreviations**

36
37 ATPB, Allyltriphenylphosphonium bromide;
38 BTPB, Benzyltriphenylphosphonium chloride;
39 ChCl, Choline chloride;
40 CAC, Choline acetyl chloride;
41 DAC, *N,N*-diethylethanolammonium chloride;
42 DES, Deep eutectic solvent;
43 EG, Ethylene glycol;
44 FT-IR, Fourier transform infrared spectroscopy;
45 Gly, Glycerol;
46 HBA, Hydrogen bond acceptor;
47 HBD, Hydrogen bond donor;
48 LA, Levulinic acid;
49 MTPB, Methyl triphenyl phosphonium bromide;
50 Pro, Propionic acid;
51 RDF, Radial distribution function;
52 RDG, Reduced density gradient
53 TBAB, Tetrabutylammonium bromide;
54 TBAC, Tetrabutylammonium chloride;
55 TBPB, Tetrabutylphosphonium bromide;
56 TEAC, Tetraethylammonium chloride.
57

58 **1. Introduction**

59 Deep eutectic solvents (DES) were designed more than a decade ago as a possible alternative to
60 ionic liquids [1]. DESs are a combination of various hydrogen bond acceptors (HBAs) and hydrogen
61 bond donors (HBDs). Thanks to some of their unique properties, they have been utilized in various
62 fields of science and technology. TBAB-based and Gly-based DESs have been applied for a variety of
63 purposes, selected examples of which are presented below.

64 The reversible absorption of SO₂ in six DESs composed of levulinic acid (LA) and various quaternary
65 ammonium salts – ChCl, CAC, TEAC, TEAB, TBAC and TBAB – at a fixed 3:1 molar ratio was studied. All
66 the examined DESs were capable of absorbing SO₂ and showed high selectivity for SO₂/CO₂. The effect
67 of water content on SO₂ absorption was also investigated. The absorption capability of the LA–ChCl
68 DES decreased slightly with increasing water content (5 and 10%), indicating a slight change in the
69 structure and efficacy of the DES. The interaction of the LA–ChCl DES and SO₂ was examined by NMR
70 and FT-IR spectroscopy, with the results showing the physical interaction between the DES and
71 dissolved SO₂ [2]. The physicochemical properties of these DESs, such as density, dynamic viscosity,
72 electrical conductivity and refractive index, were later investigated [3]. Wu et al. investigated the
73 absorption capability of H₂S of two series of DESs based on TBAB or ChCl as the HBA with carboxylic
74 acids (formic acid, acetic acid and propionic acid) as the HBD at various molar ratios. The solubility of
75 H₂S increased with decreasing carboxylic acid concentration in the DES and was higher for TBAB-based
76 DESs compared to ChCl-based ones, with TBAB:Pro showing the best results [4]. Hizaddin et al. [5]



77 investigated the extractive denitrogenation of diesel fuel using ammonium- and phosphonium-based
78 DESs (TBAB and TBPB) and ethylene glycol at a 1:2 molar ratio. The DESs were tested to remove 5-
79 membered nitrogen compounds (pyrrole and indoline) and 6-membered nitrogen compounds
80 (pyridine and quinoline) from a model diesel compound (n-hexadecane). Phosphonium-based DESs
81 show higher values of the distribution coefficient (D) and selectivity (S) than ammonium-based ones
82 towards nitrogen compounds. Moreover, the investigated DESs have higher values of D and S towards
83 5-membered nitrogen compounds than for 6-membered ones [5]. Aqueous bi-phasic systems based
84 on TBAB-based DESs were developed and applied in the rapid extraction of DNA from salmon testes.
85 Four DESs based on TBAB and ethylene glycol, propylene glycol, butylene glycol and butyl alcohol were
86 synthesized and tested. TBAB-EG and sodium sulfate were selected as the appropriate phase
87 components. The interaction between DNA and the DES was confirmed by FT-IR spectra, circular
88 dichroism spectra, dynamic light scattering and transmission electron microscope [6].

89 A few papers can be found devoted to the study of the physical properties of TBAB-Gly DESs. Yusof
90 et al. studied the effect of HBD percentages, HBD type and temperature on the density, viscosity and
91 ionic conductivity of DESs formed by TBAB with alcohol-based HBDs (ethylene glycol, 1,3-propanediol,
92 1,5-pentanediol and glycerol). DESs based on TBAB-glycerol had the highest density and viscosity and
93 the lowest ionic conductivity when compared to other DESs, probably due to the extra hydroxyl group
94 of glycerol [7]. The physical properties (freezing point, density, viscosity, conductivity, and surface
95 tension) of six DESs based on glycerol as the HBD and six different salts (MTPB, BTPB, ATPB, ChCl, DAC,
96 TBAB) at various molar ratios of the HBD to the salts were studied. Ammonium-based salt DESs had
97 much lower viscosities than phosphonium-based salt DESs. Within the ammonium group, the
98 viscosities of the different DESs increased as their molecular weights increased [8].

99 Besides the physicochemical properties of DESs, their formation mechanisms are quite significant
100 for further application. It's well-known that hydrogen bonds between the HBA and the HBD play a
101 dominant role in eutectic mixture formation. In order to identify H-bonds, spectroscopic methods,
102 including FT-IR and NMR, are typically used [8,9]. As observed in other work, weaker non-bonded
103 interactions can also determine DES formation [10]. In a previous work [11], we reported the NMR, IR
104 and Raman spectra of a TBAB-Gly-based DES at various HBA:HBD molar ratios for neat DES as well as
105 a DES with various amounts of water added. However, it is very difficult to identify these interactions
106 through experimental methods [12–14]. For this purpose, a theoretical quantum mechanical
107 calculation, which is a forceful tool for simulating molecular structures, can be used. However, only
108 the combination of experimental and theoretical research enables complete insight into DES formation
109 [15]. Therefore, herein we report the theoretical quantum mechanical calculations of
110 tetrabutylammonium bromide-glycerol-based deep eutectic solvents and their mixtures with water.
111 The simulations presented in the paper fully complement the previous experimental work [11].

112 2. Computational studies

113 The theoretical analysis of deep eutectic solvents composed of tetrabutylammonium bromide and
114 glycerol in various molar ratios (1:2, 1:3, 1:4) and DES-water complexes were studied based on previous
115 studies [10,16–20]. All the calculations, including molecular structure optimization and vibrational
116 frequencies of the TBAB, Gly, water and DES, were performed based on the Beck3-Lee-Yang-Parr
117 (B3LYP) level with the use of the 6-31+G** basis set. This basis set is large enough to calculate the
118 vibrational frequencies and structure of deep eutectic solvents composed of TBAB and Gly in various
119 molar ratios [21,22]. All the optimized configurations of deep eutectic solvents were tested to be local

120 minima by frequency calculations. The interactions energy (ΔE) between the HBA and HBD in the DES
121 molecule was calculated from equation (1):

$$122 \quad \Delta E = E_{DES} - (E_{HBA} - E_{HBD}) \quad (1)$$

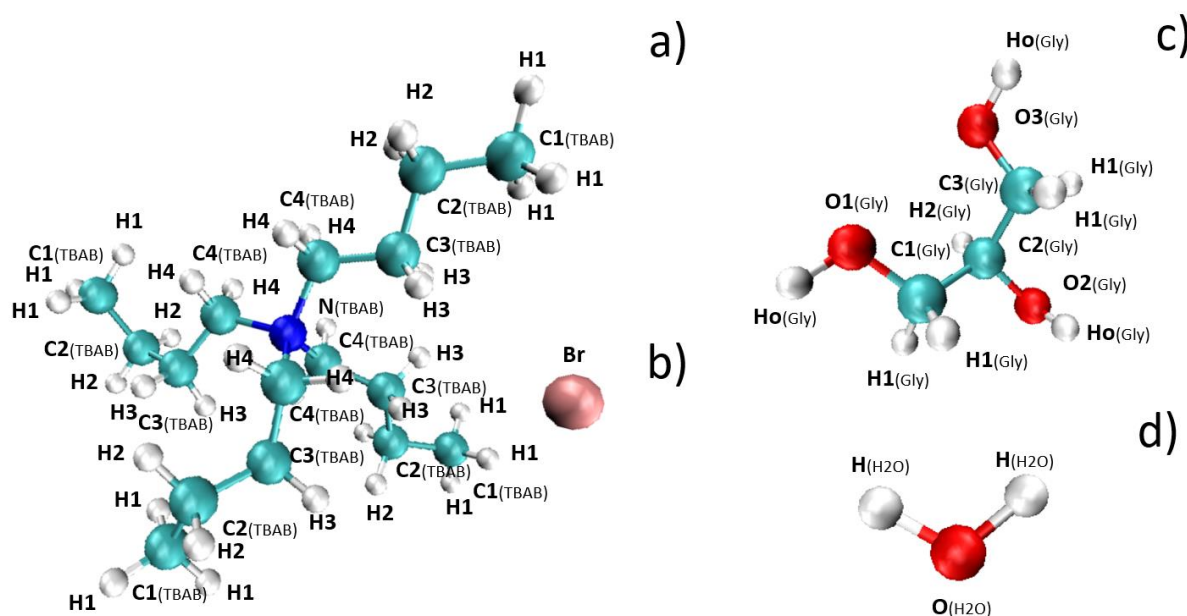
123 Where: E_{DES} is the total energy of DES composed of the HBA and HBD [kcal/mol], and E_{HBA} , and E_{HBD} are
124 the individual energies of the HBA and HBD, respectively [kcal/mol].

125 The interactions energy between the DES composed of TBAB and Gly in a 1:3 molar ratio and
126 water was calculated according to the equation (2):

$$127 \quad \Delta E = E_{DES-H_2O} - (E_{DES} - E_{H_2O}) \quad (2)$$

128 where: E_{DES-H_2O} is the total energy of the complex composed of the DES and water [kcal/mol], and E_{DES}
129 and E_{H_2O} are the individual energies of the DES and water [kcal/mol].

130 The counterpoise procedure was used to account for the basis set superposition error (BSSE)
131 [23]. The structures and atom definitions of DESs are presented in the Figure 1.



132
133 **Figure 1** Geometries of a) tetrabutylammonium cation; b) bromide anion; c) glycerol; d) water.

134 For better discussion of the nature of the interactions between the HBA and HBD, as well as
135 between the DES, a reduced density gradient (RDG) was applied. The RDG analysis was made using the
136 Multiwfn software [24–26]. The Visual Molecular Dynamics 1.9.3. software was used to graphically
137 present the results. In the further studies, for the pure DES in 1:2, 1:3, and 1:4 molar ratio, 100 TBAB
138 and 200, 300, and 400 Gly molecules, were introduced onto a box, defined by the minimum
139 coordinates x, y and $z = 0, 0, 0$ and maximum coordinates 40, 40, 40. The distance tolerance between
140 atoms was 2.0 Å. In the next step, 100 TBAB:Gly (1:3) molecules and water molecules were placed in
141 the box (Table 1), using PackMol code [27]. All computational studies were performed at constant
142 pressure (1 bar) using Parrinello–Rahman barostat [28] and constant temperature (293.15 K) by means
143 of Nose–Hoover thermostat [29,30] for the equilibration of all of the systems for 20–25 ns. In the
144 simulations, a 10 ns production run was carried out with a trajectory saving frequency of 0.1 ps to

145 compute structural properties of all studied systems. Force field parameters were derived from OPLS-
 146 AA model. In addition, the rigid SPC/E model was adopted for water molecules [31]. The presented
 147 simulations were performed by means of GROMACS 2020.5 software [32,33].

148 **Table 1** Compositions of DES-H₂O complexes investigated in the present work

DES-H ₂ O complex	Number of molecules		
	TBAB	Gly	H ₂ O
TBAB:Gly (1:3)	100	300	0
80% TBAB:Gly (1:3)-20%H ₂ O	100	300	100
50% TBAB:Gly (1:3)-50%H ₂ O	100	300	200
20% TBAB:Gly (1:3)-80%H ₂ O	100	300	700
10% TBAB:Gly (1:3)-90%H ₂ O	100	300	2300

149

150 3. Results and Discussion

151

152 3.1. Deep eutectic solvents structures

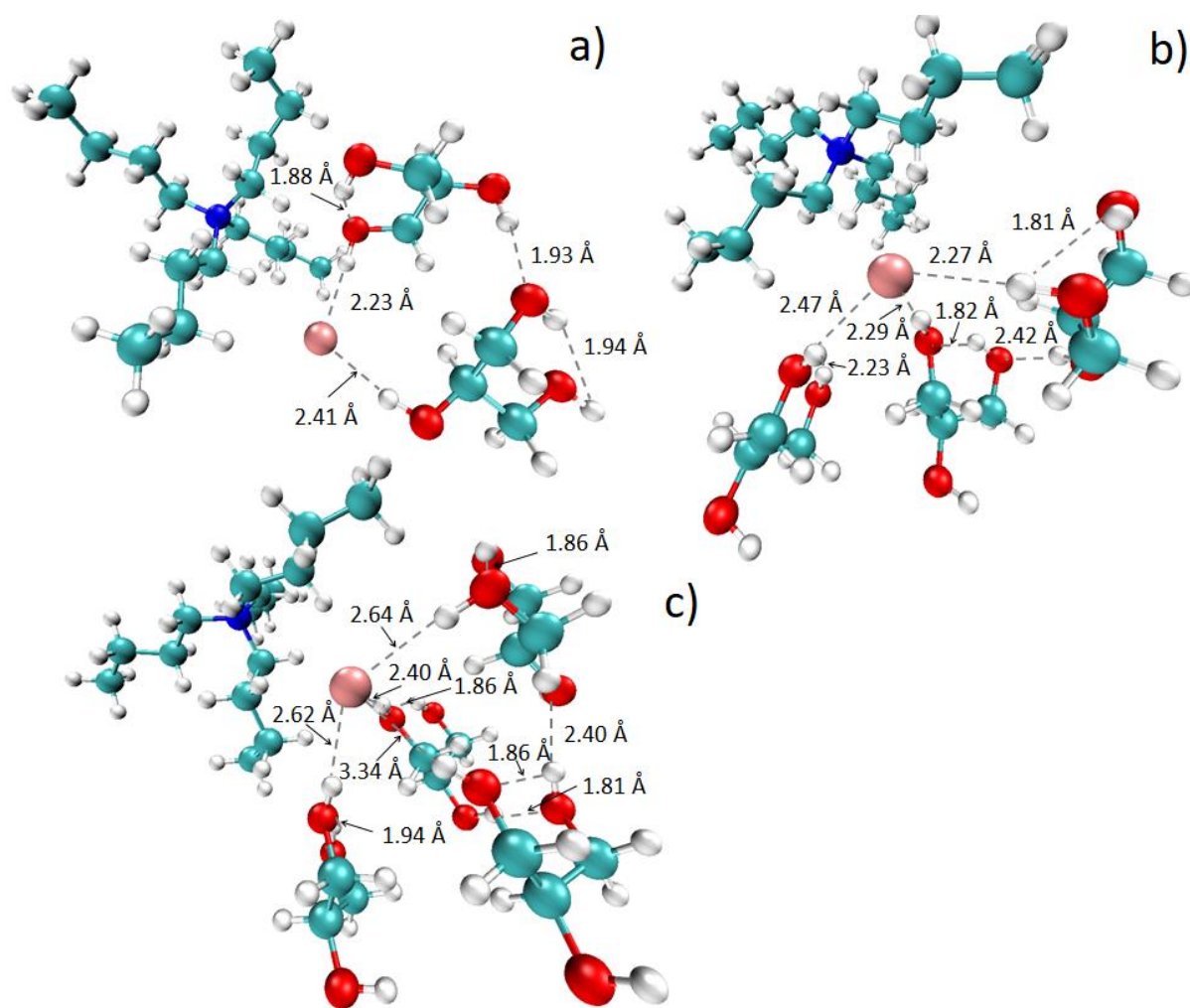
153

154 Information of mechanism of DES (TBAB:Gly in 1:2, 1:3, 1:4 molar ratios) formation and influence
 155 of water addition on the DES structures which were obtained from the previous studies based on
 156 spectroscopic analysis i.e. Raman, FT-IR, ¹H NMR, ¹³C NMR are not unambiguous, and they only
 157 indicate the existence of strong hydrogen bonds between the hydrogen bond donors and hydrogen
 158 bond acceptors [11]. However, they do not indicate the number of hydrogen bonds, their exact
 159 location and information on weaker interactions, i.e. the electrostatic interactions in the DES
 160 structures. Therefore, theoretical studies of were carried out to better understand the mechanism of
 161 DES formation.

162 The most stable and probable complexes in the gas phase of TBAB:Gly (1:2); TBAB:Gly (1:3);
 163 TBAB:Gly (1:4) were geometry optimized at the B3LYP/6-31+G** level of theory. The results of
 164 geometry optimization of the DES complex are presented in Figure 2. The geometric results show that
 165 in all DES configurations, nonbonded interaction exists between the Br atom from TBAB and Gly
 166 molecules, which can be identified as strong hydrogen bonds because of the short distances between
 167 the atoms (below 2.5 Å) [34]. In the TBAB:Gly (1:2) structure, the distances between the Br atom and
 168 the hydroxyl groups from the glycol O-H...Br are 2.23 Å and 2.41 Å. In TBAB:Gly (1:3) these distances
 169 are 2.27 Å, 2.29 Å and 2.47 Å and in TBAB:Gly (1:4) 2.64 Å, 2.40 Å, 2.62 Å and 1.86 Å. This indicates that
 170 with increasing glycerol content in the DES, the hydrogen bonds between the HBA and HBD weaken
 171 (O-H...Br). In addition, strong hydrogen bonds can be identified between the -OH groups in the
 172 glycerol molecules. The distances O-H...H-O are 1.93 Å in TBAB:Gly (1:2), 2.42 Å in TBAB:Gly (1:3) and
 173 1.81 Å and 2.40 Å in TBAB:Gly (1:4). In all Gly molecules, intramolecular hydrogen bonds (O-H...H-O)
 174 occur for which the distances are in range from 1.81 to 2.23 Å. In all complexes the distance between
 175 the TBAB molecule and the Gly molecules is higher than 2.5 Å, which indicates that other weaker, non-
 176 covalent interactions exist.

177 Under real conditions, a DES composed of TBAB and Gly in a 1:2 molar ratio is solid at room
 178 temperature, which indicates that two H-bonds between the HBA and HBD is not enough for the
 179 formation of the eutectic mixture. TBAB:Gly (1:3) is a liquid with a tendency to crystallize after a few
 180 days. This shows that the three H-bonds between TBAB and Gly are a minimum for the formation of a
 181 liquid complex. On the other hand TBAB:Gly (1:4) is a liquid at room temperature and contains only

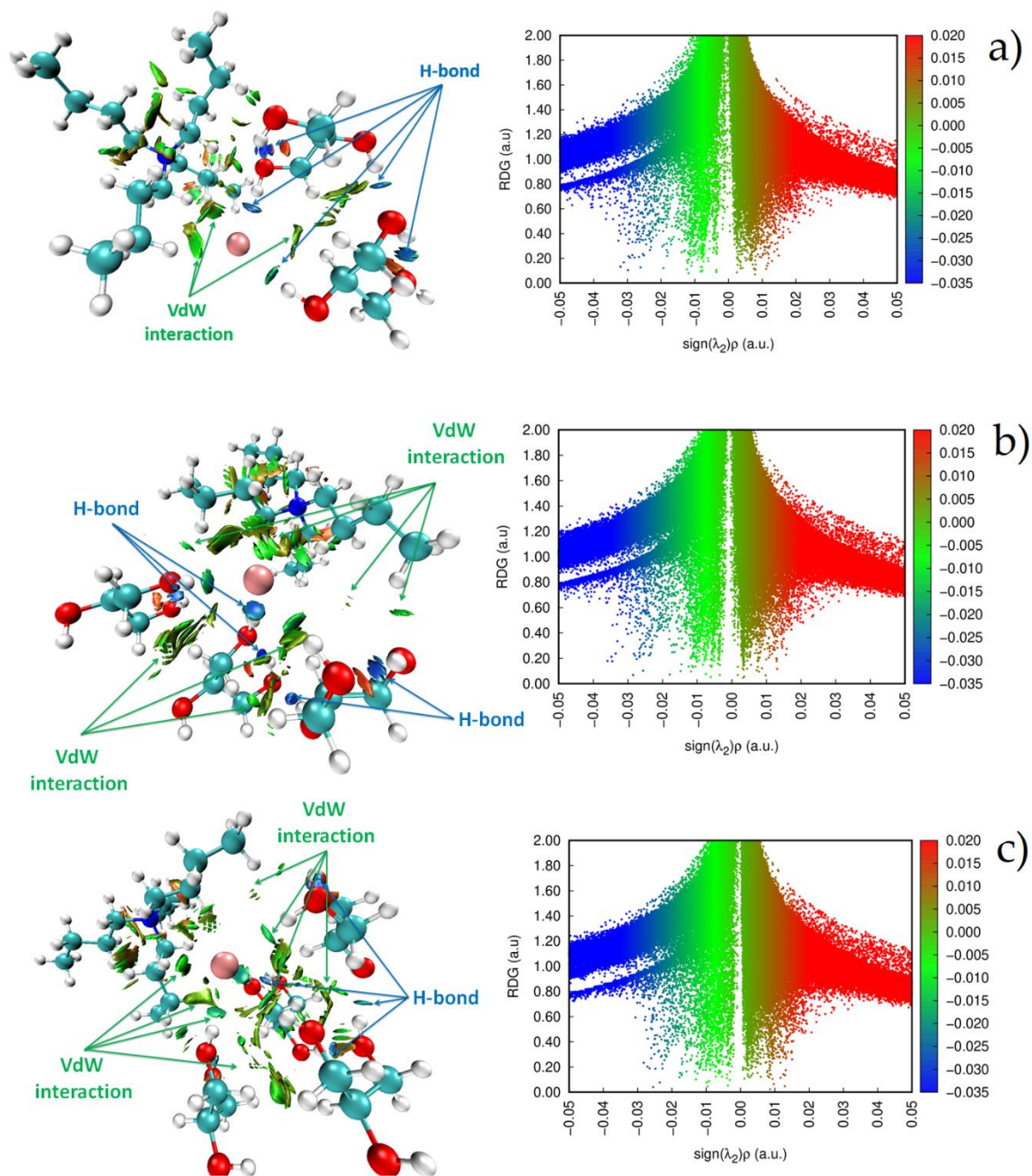
182 two hydrogen bonds between the HBA and HBD, which indicates that the hydrogen bonds between
183 the Gly molecules also play a main role in eutectic mixture formation.
184



185
186 **Figure 2** Optimized structures of a) TBAB:Gly (1:2); b) TBAB:Gly (1:3); TBAB:Gly (1:4).
187

188 To better describe the nature of the intermolecular interaction of the DESs and to confirm the
189 existence of hydrogen bonds between the HBA and HBD, the reduced density gradient (RDG) method
190 was employed. RDG is a useful method for detecting weak interactions based on electron density and
191 its derivatives. It enables identification of both strong hydrogen bonds and van der Waals interactions,
192 as well as steric repulsion in molecules [26]. A graphical interpretation of the obtained results is
193 presented in Figure 3, where blue areas represent strong attractive effects (hydrogen bond); red areas
194 indicate strong repulsive interactions; and green areas denote weaker noncovalent interactions,
195 including van der Waals interaction. The obtained results show that in TBAB:Gly (1:2) two hydrogen
196 bonds between the Br atom and the –OH groups from Gly, two intermolecular H-bonds in Gly
197 molecules, as well as one hydrogen bond between the hydroxyl group from Gly existed, which
198 correspond to the negative $\text{sign}(\lambda^2)\rho$ value (from -0.04 to -0.02 a.u.) in the 2D diagram (Figure 3). In
199 addition, van der Waals interactions also occurred in the TBAB:Gly (1:2) complex between the HBA and
200 HBD with 0.01 a.u. $< \text{sign}(\lambda^2)\rho < 0.01$ a.u. values. The same interactions exist in TBAB:Gly (1:3) and
201 TBAB:Gly (1:4). However, there are no additional hydrogen bonds, and only weaker van der Waals

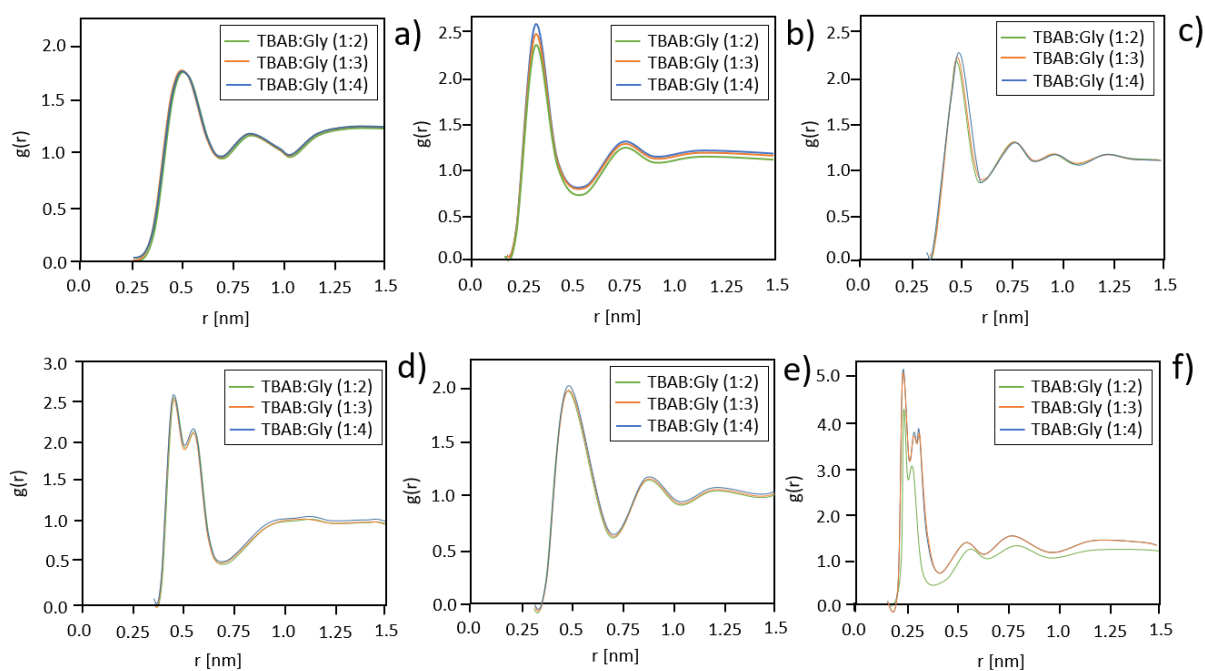
202 interactions exist between the third and fourth Gly molecule and the Br atom, as well as between the
 203 Gly molecules. The coexistence of both types of non-bonded interactions, i.e. hydrogen bonds and van
 204 der Waals interaction between TBAB and Gly molecules, corresponds to the formation of a stable deep
 205 eutectic solvent complex.



206
 207 **Figure 3** Reduced density gradient isosurfaces ($s = 0.5$ a.u.) and 2D diagrams of electron density and its reduced
 208 density gradient for a) TBAB:Gly (1:2); b) TBAB:Gly (1:3); c) TBAB:Gly (1:4).
 209

210 In order to study the interactions between DES components in larger systems, the center of mass
 211 Radial distribution functions (RDF) were studied (Figure 4). The obtained results indicate that the
 212 increase in the numbers of Gly molecules in the DES-complexes practically does not weaken TBA⁺-TBA⁺
 213 and TBA⁺-Gly correlations, because the shifts and decrease first peaks intensity is not observed (Figure

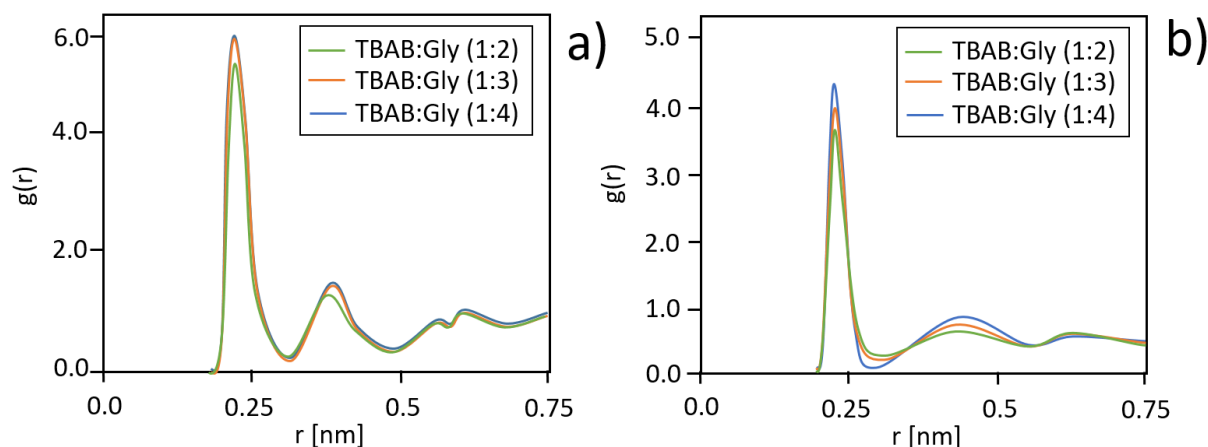
214 4 a,e). An increase in the number of Gly in DES causes an increase in the intensity of the peaks and a
 215 shift of the peaks towards lower values in Gly–Gly and Br–Gly molecules. This indicates that additional
 216 hydrogen bonds are being formed between the glycols (Gly–Gly) within DES or between DES molecules
 217 (Figure 4b), as well as between Br– and Gly in DES structure (Figure 4f). However, in Br–Gly correlation
 218 the increase in peak intensity is observed after the addition of three Gly molecules, while after the
 219 addition of four Gly molecules to the DES structure, the intensity of peak does not change. This
 220 indicates that there are no additional strong interactions (i.e. hydrogen bonding) between Br and Gly
 221 after a further increase in numbers of Gly molecules. It can be assumed that further increasing the Gly
 222 in the DES structure would result in the formation of glycerol dimers. In contrast the inverse
 223 relationships can be observed for Br[–]–Br[–] and TBA⁺–Br[–] systems. This indicates that Br[–]–Br[–] and TBA⁺–
 224 Br[–] correlations become weaker and the nearest neighbor distance between ions increases with the
 225 increase of Gly molecules in DES systems. In all DES systems, correlation of Gly–Br[–] is more prominent
 226 than TBA⁺–Br[–], which indicate that the Gly–Br play an important role in DES formation, which was also
 227 observed in another DES complex [19,20,35].
 228



229
 230 **Figure 4** Intermolecular center of mass Radial distribution functions (RDF) for a) TBA⁺–TBA⁺; b) Gly–Gly; c) Br[–]–
 231 Br[–]; d) TBA⁺–Br[–]; e) TBA⁺–Gly; f) Br[–]–Gly.

232
 233 The atomic RDF enables the identification of hydrogen bonds between molecules in large DES
 234 systems. Based on the previous experimental studies [11] and geometric optimization of the simple
 235 single DES structures, it can be concluded that in DES molecule, the three types of hydrogen bonds exist
 236 (between hydroxyl group from Gly and Br[–], between hydroxyl groups from Gly molecules (Gly–Gly)
 237 within DES, and intermolecular O–H···H–O in the Gly structure). However, in DES formation process
 238 only two types of H-bonding play a dominant role (Br[–]···HO_(Gly) and OH_(Gly)···HO_(Gly)). Therefore, in further
 239 studies these two types of interactions were taken into account. The results of atomic RDF indicate that
 240 the first peak in Br[–]···HO_(Gly) correlation, slightly shifts towards a lower distance value in TBAB:Gly (1:3)

241 relative to TBAB:Gly (1:2) (Figure 5). In addition, the increase of intensity of the first peak can be
 242 observed after an increase of Gly content in the DES structures. However, further addition of Gly
 243 molecules in the DES structure does not provide any change in the atomic RDF chart. The peaks in both
 244 systems almost overlap. This indicates that despite the addition of an additional Gly molecule, no
 245 additional hydrogen bonds are formed between $\text{OH}_{(\text{Gly})}-\text{Br}$. On the other hand, shifts of the first peak
 246 towards lower values and an increase in peak intensity after increasing the Gly content in the DES
 247 structure, indicate the formation of hydrogen bonds between glycol molecules. This probably leads to
 248 the formation of Gly dimers.
 249



250

251 **Figure 5** Atomic Radial distribution functions (RDF) for a) $\text{Br}^- - \text{HO}_{(\text{Gly})}$, b) $\text{HO}_{(\text{Gly})} - \text{HO}_{(\text{Gly})}$.

252 3.2. Mixtures of deep eutectic solvents and water

253

254 In the next part of studies, simple single molecule system TBAB:Gly (1:3) with the addition
 255 of one, two, seven and twenty-three water molecules which represent the DES:H₂O 20:80%,
 256 50:50%; 80:20% and 90:10% volumetric ratio, were analyzed. **The experimental density values**
 257 **at 20°C are 1.145, and 1.029, 1.072, 1.116, 1.131 g / cm³ respectively for pure TBAB: Gly (1: 3)**
 258 **and DES-water complexes in 20:80%, 50:50%; 80:20% and 90:10% v/v.** After the addition of
 259 water, the distances between the Br^- and the $-\text{OH}$ groups from glycerol become longer. This
 260 indicates that the hydrogen bonds between the HBA and HBD become weaker, which the
 261 theoretical and experimental FT-IR and Raman spectroscopy results confirm [11]. The detailed
 262 $\text{O}-\text{H}\cdots\text{Br}$ distances are presented in Table 2.

263

264

265

266

267

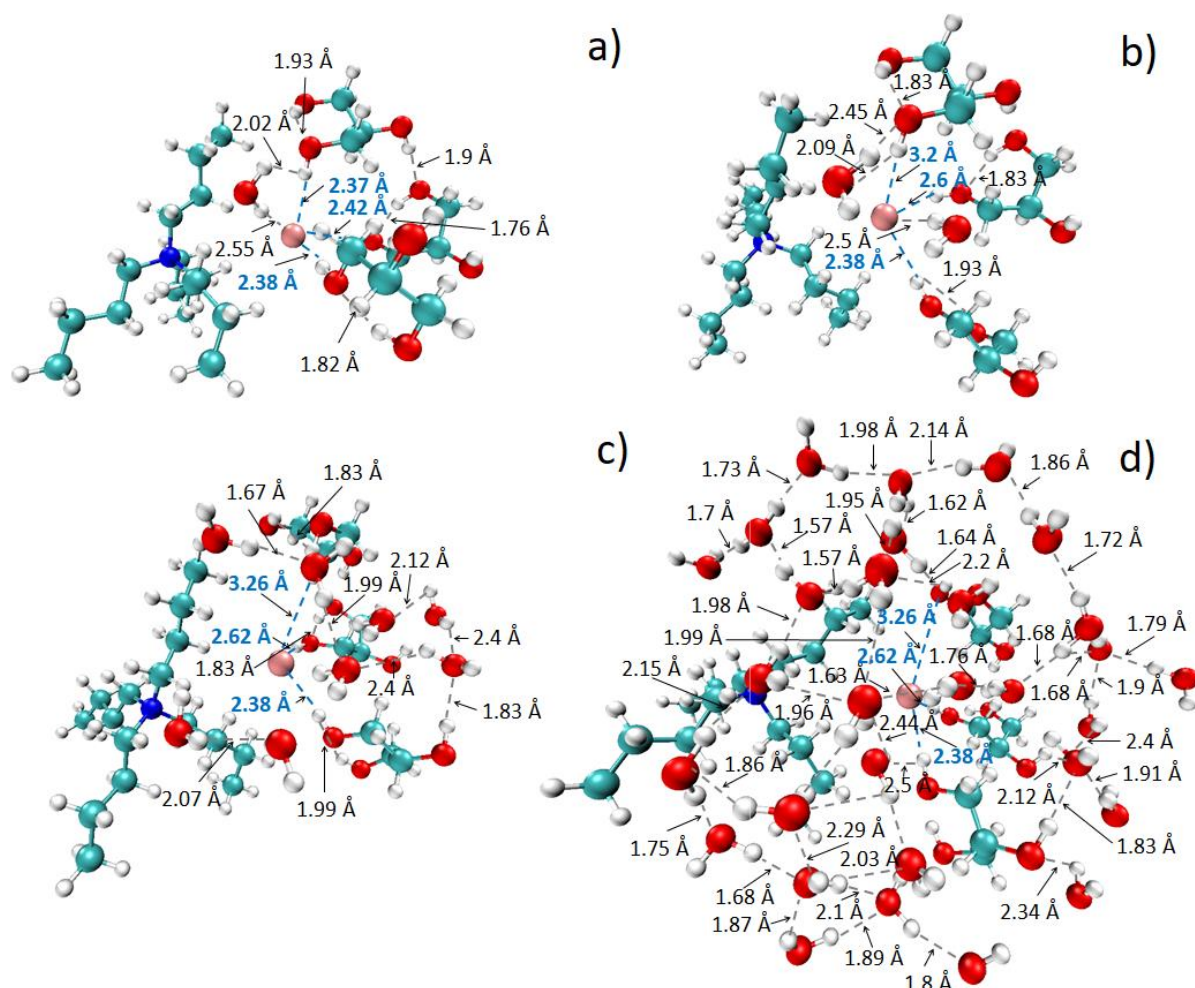
268

269

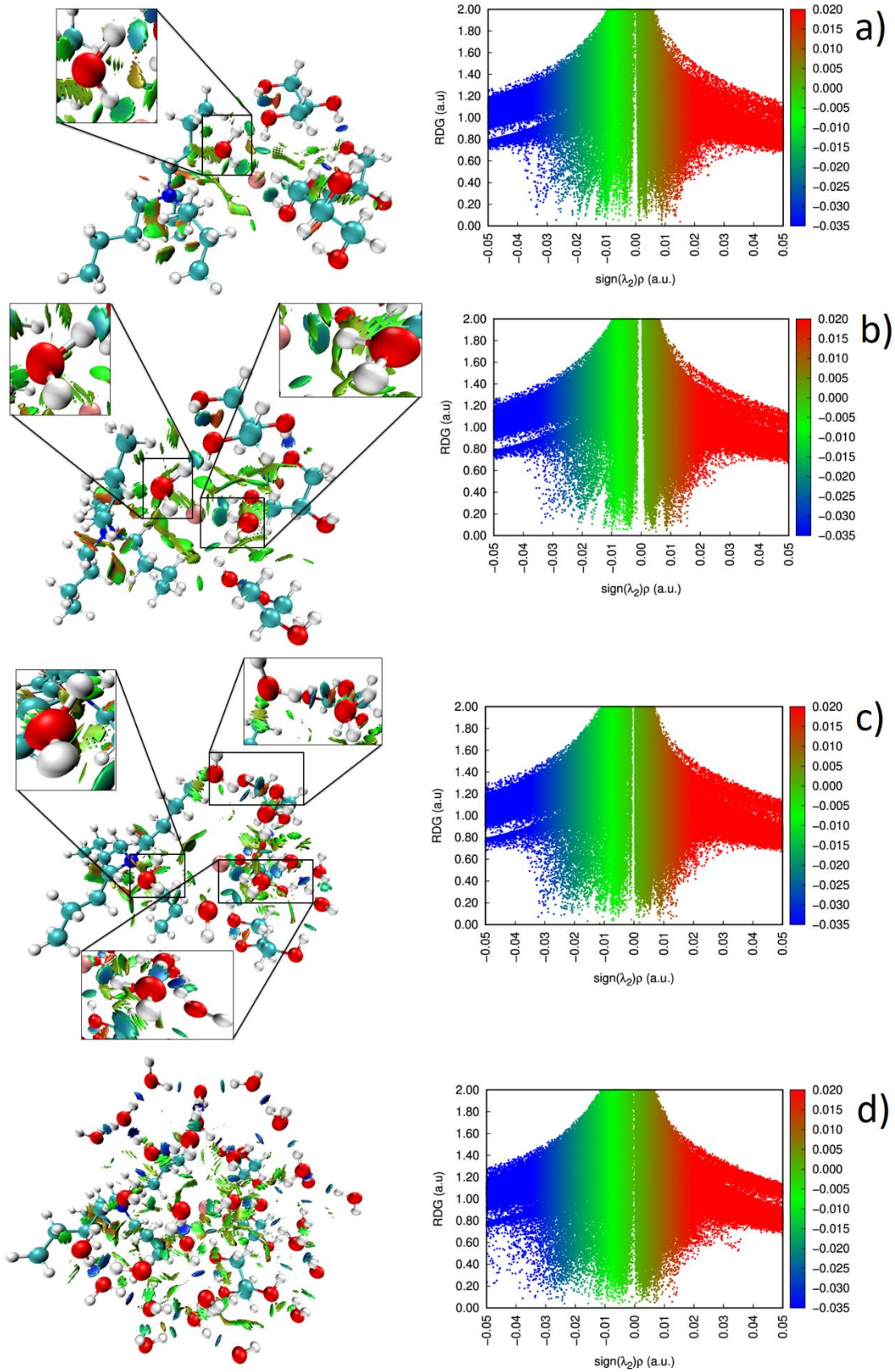
270 **Table 2** Distances between the Br atom and the –OH group from glycerol components [Å]. The (1), (2),
 271 and (3) represent the number of the glycerol molecule that is involved in the hydrogen bond formation
 272 with HBD.

Complex	(1) O–H···Br	(2) O–H···Br	(3) O–H···Br
TBAB:Gly (1:3)	2.27	2.47	2.29
80% TBAB:Gly (1:3)–20% H ₂ O	2.37	2.42	2.38
50% TBAB:Gly (1:3)–50% H ₂ O	3.20	2.60	2.60
20% TBAB:Gly (1:3)–80% H ₂ O	3.26	2.62	2.68
10% TBAB:Gly (1:3)–90% H ₂ O	3.26	2.62	2.79

273 On the other hand, new strong hydrogen bonds with distances below than 2.5 Å between the –
 274 OH groups from water and glycerol (O–H···O–H) and water and water (O–H···O–H), as well as weaker
 275 bonds between the Br atom and the hydroxyl groups from water (O–H···Br) with distances higher than
 276 2.55 Å appeared. A graphical presentation of the optimized structures of DES-water complexes with
 277 distances between functional groups and reduced density gradient isosurfaces are presented in Figures
 278 6 and 7.
 279



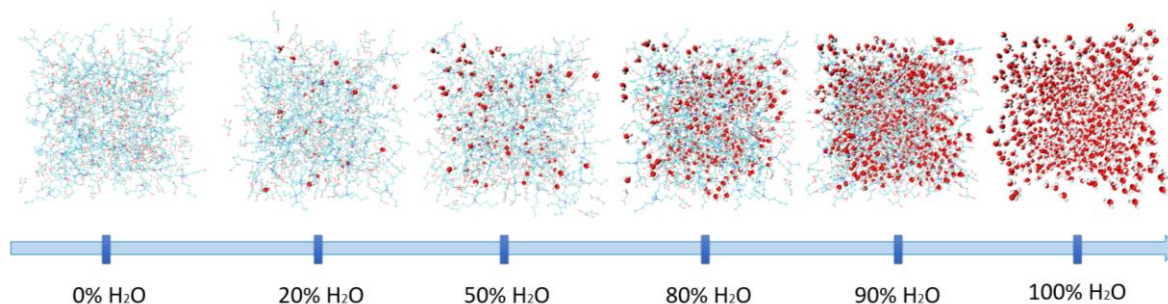
280
 281 **Figure 6** Optimized structures of a) 80% TBAB:Gly (1:3)–20% H₂O; b) 50% TBAB:Gly (1:3)–50% H₂O; c) 20%
 282 TBAB:Gly (1:3)–80% H₂O; d) 10% TBAB:Gly (1:3)–90% H₂O
 283



284

285 **Figure 7** Reduced density gradient (s = 0.5 a.u.) and 2D diagrams of electron density and its reduced
 286 density gradient for a) 80% TBAB:Gly (1:3)–20% H₂O; b) 50% TBAB:Gly (1:3)–50% H₂O; c) 20% TBAB:Gly (1:3)–
 287 80% H₂O; d) 10% TBAB:Gly (1:3)–90% H₂O

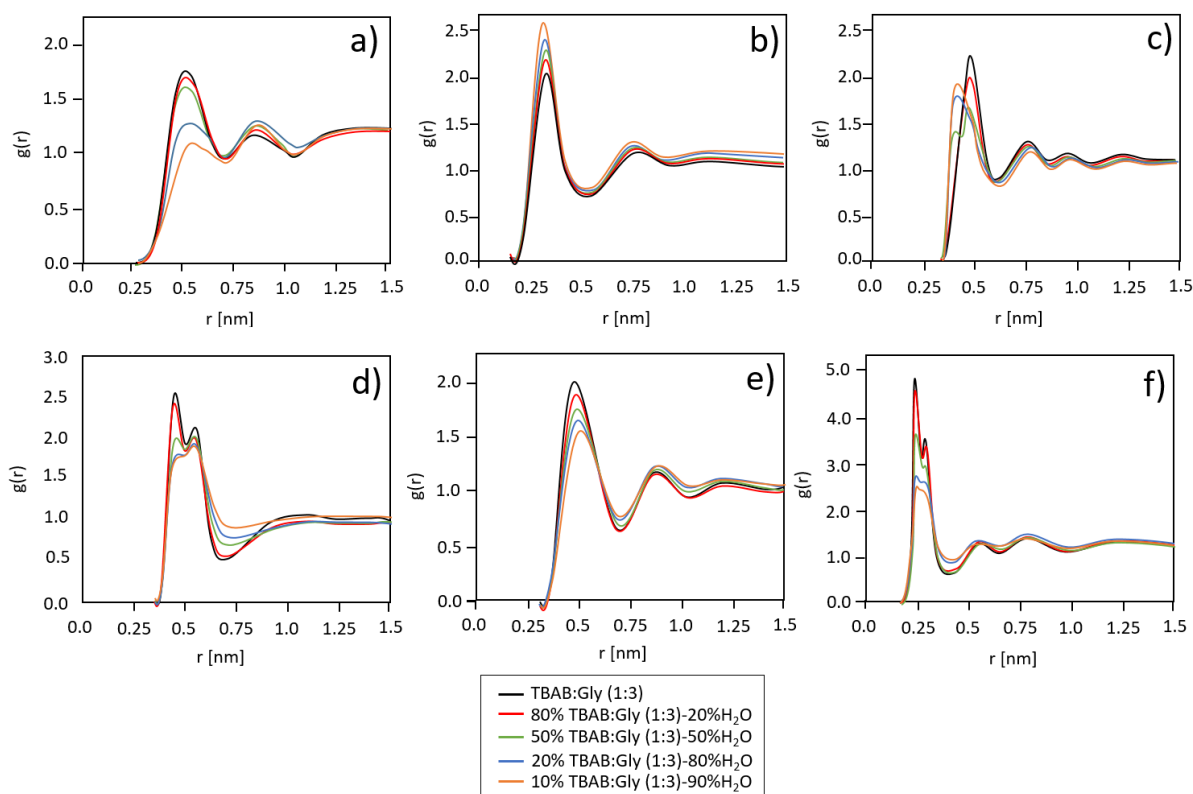
288 In order to explain of the influence of water addition on the intermolecular interactions of
289 large DES complexes, the center of mass Radial distribution functions (RDF) were studied. The
290 snapshots of TBAB:Gly (1:3)-water complexes are presented in the Figure 8.



291

292 **Figure 8** Snapshots of TBAB:Gly (1:3)-water mixtures represents various amount of water.

293 The results presented in Figure 9 indicate that $TBA^+ - TBA^+$, $TBA^+ - Br^-$, $Gly - Br^-$ correlation in
294 large DES-water systems as expected, becomes weaker with the volume of water addition. In all
295 correlations, a decrease in the intensity of the first peak can be observed. However, only in $TBA^+ - TBA^+$
296 correlation shifts of the first solvation peak towards a longer length are observed. In the rest of
297 correlation, the position of peaks doesn't not change its position. This indicates a lower effect of the
298 water addition on $TBA^+ - Br^-$, and $Gly - Br^-$ compared to $TBA^+ - TBA^+$ pairs. In turn, with the addition of
299 water, an increase in peak intensity and its shift towards lower distances in $Gly - Gly$ and $Br^- - Br^-$
300 correlations can be observed. This indicates that Gly molecules and bromide atoms, come closer in the
301 presence of water in comparison to pure DES. This is probably due to the fact that water even at low
302 concentration is a strong ligand for bromide binding and out-competing DES species due to its
303 hydrogen bonding capability, as well as small molecular volume. Water molecules occupy the space
304 around bromine atoms, which provide to reduce $Br^- - Br^-$ separation via bridging in solvent-separated
305 pairs [20]. Similar results were also observed in other works dedicated to DES- H_2O complexes
306 composed of choline chloride:glycolic acid [20], and choline chloride:urea [19,20,35] which proved that
307 the addition of a small amount of water (5-10%) can stabilize the DES network.



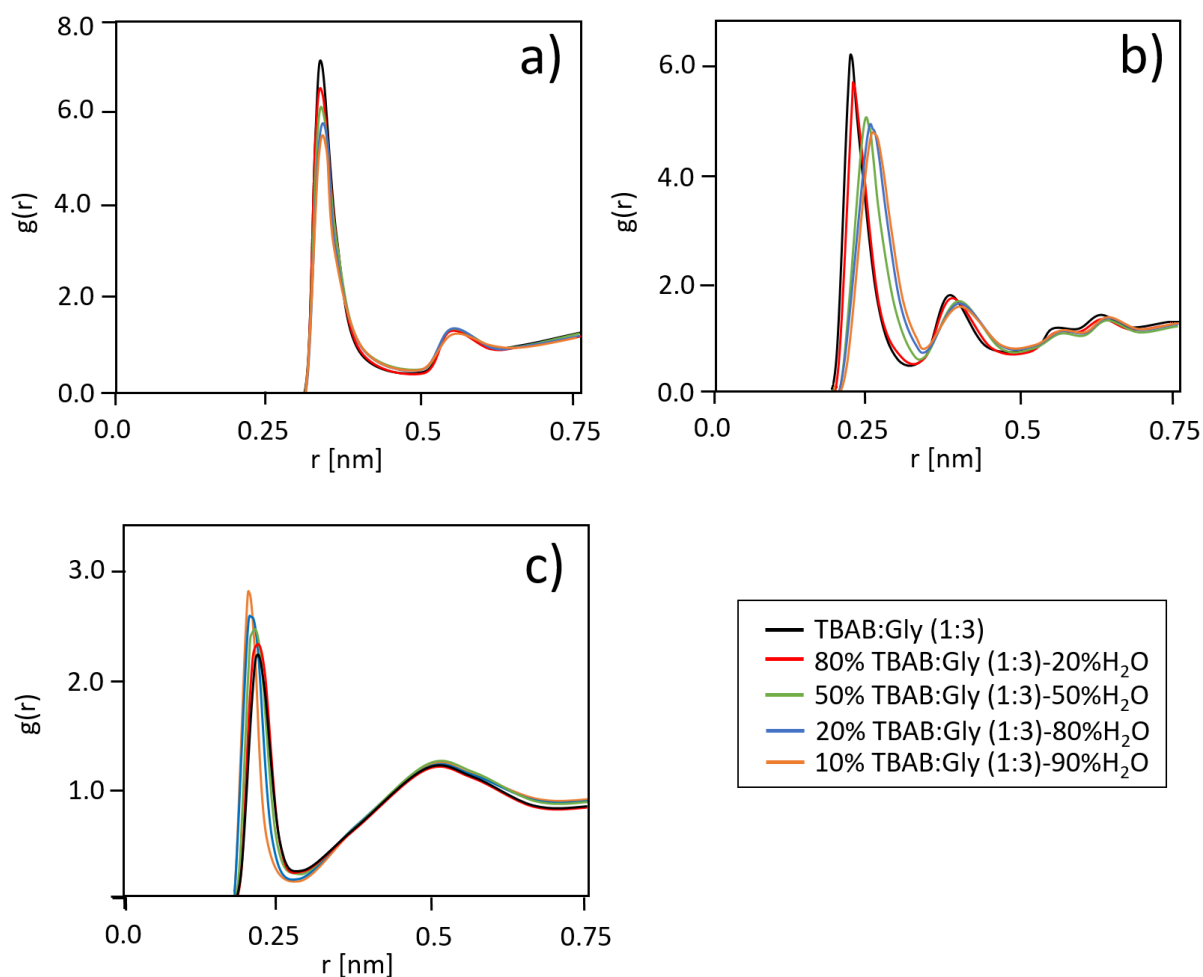
308
 309 **Figure 9** Intermolecular center of mass Radial distribution functions (RDF) for a) TBA⁺–TBA⁺; b) Gly–Gly; c) Br[–]–
 310 Br[–]; d) TBA⁺–Br[–]; e) TBA⁺–Gly; f) Br[–]–Gly in DES-water systems.

311

312 In the next part of the studies, atomic RDF was used to explain how the addition of water
 313 affects the hydrogen bonding in DES structures in large systems (Figure 10). The obtained results
 314 indicate the decreasing propensity of Br[–] atom to the formation of H-bonding with the hydroxyl group
 315 from Gly with increasing water volume in DES-H₂O systems. The first solvation peak shifts towards the
 316 higher values from about 0.23 to 0.26 nm after the addition of 50% (v/v). Based on the shifts, it can
 317 be concluded that typical Br[–]⋯HO_(Gly) hydrogen bonds are destroyed with the addition of minimum 50%
 318 (v/v) of water. A further increase in the volume of water causes a further extension of the distance
 319 between the Br atom and the hydroxyl groups of Gly (Figure 10). This is probably due to the fact that
 320 the water molecules are strong hydrogen-bond donors which provide for enhanced involvement of Br[–]
 321 water interactions. The similar results were obtained for another atom pair i.e. N_(TBAB)–Br[–]. On the other
 322 hand, the first solvation peak shifts towards the lower distance values in HO_(Gly)⋯HO_(Gly), after water
 323 addition can be observed, which is in line with the above considerations. The similar results was
 324 observed for the complex of water and DES composed of choline chloride and ethylene glycol [19].

325

326



327

328 **Figure 10** Atomic Radial distribution functions (RDF) for a) $N_{(TBAB)}-Br^-$; b) $OH_{(Gly)}-Br^-$; c) $OH_{(Gly)}-HO_{(Gly)}$.

329 The interaction energy between the HBA and HBD, as well as between the DES and water
 330 molecules in most cases is negative, and the lower values indicate stronger interactions inside the
 331 complex. The list of calculated interaction energies is presented in Table 3. The calculated values of
 332 the DES complexes followed a similar trend as the experimental data: TBAB:Gly (1:3) ~ TBAB:Gly (1:4)
 333 < TBAB:Gly (1:2). Despite the weakening of the hydrogen bonds between the HBA and HBD after the
 334 addition of water, stronger interaction energies occurred in 10% TBAB:Gly (1:3)–90% H₂O. This is
 335 caused by numerous water molecules and the formation of large amounts of hydrogen bonds between
 336 them. Along with reduction of the water content in the complexes, the strength of the interaction
 337 energy decreases.

338 **Table 3** Interaction energies between HBA and HBD as well as between DES and water

Complex	Interaction energy [kcal/mol]
TBAB:Gly (1:2)	-9.6
TBAB:Gly (1:3)	-11.2
TBAB:Gly (1:4)	-11.0
80% TBAB:Gly (1:3)-20% H ₂ O	-12.1
50% TBAB:Gly (1:3)-50% H ₂ O	-16.2
20% TBAB:Gly (1:3)-80% H ₂ O	-18.1
10% TBAB:Gly (1:3)-90% H ₂ O	-19.5

339

340 4. Conclusion

341 In the present paper, the results of experimental ^1H NMR, ^{13}C NMR, FT-IR and Raman spectroscopy
342 studies of three deep eutectic solvents composed of TBAB and Gly in 1:2, 1:3 and 1:4 molar ratios
343 published very recently [11] were compared with theoretical studies by means of quantum mechanical
344 calculations. In addition, the influence of the varying amounts of added water on the DES structures
345 was also examined using the same procedures. The specific conclusions are as follows:

- 346 - The obtained experimental and calculated NMR, FT-IR and Raman spectroscopy results
347 indicate that the hydrogen bonds between TBAB and Gly exist in all the DESs [11]. However, it
348 was difficult to detect how many and where the hydrogen bonds occur. Identification of the
349 number and location of the H-bonds was possible using quantum mechanics calculations. The
350 results of the QM calculations indicate that three type of H-bonds exist in the DES structures,
351 including $\text{O}-\text{H}\cdots\text{Br}$ between Br and Gly, intermolecular $\text{O}-\text{H}\cdots\text{H}-\text{O}$ in the Gly structure, and $\text{O}-$
352 $\text{H}\cdots\text{H}-\text{O}$ between the Gly molecules.
- 353 - All three types of H-bonds can influence the DES. The number of hydrogen bonds depends on
354 the number of Gly molecules used in the synthesis of the DES. The total number of H-bonds
355 were 5, 7 and 7, in TBAB:Gly (1:2), TBAB:Gly (1:3) and TBAB:Gly (1:4), respectively. This
356 indicates that an increase in Gly molecules (over three Gly molecules) in the DES structures
357 does not increase the number of hydrogen bonds. On the other hand, the complete liquid state
358 of TBAB:Gly (1:4) in comparison to the other DESs indicates that not only H-bonds but also
359 weaker non-bonded interactions, i.e. van der Waals, play an important role in the eutectic
360 mixture formation.
- 361 - The small addition of water provides the formation of stable complex TBAB:Gly (1:3)–water.
362 However, a further increase in water content (higher than 50% v/v) provide to the destruction
363 of the most important hydrogen bonds ($\text{O}-\text{H}\cdots\text{Br}$) in DES structure.

365 Acknowledgements

366 V.A. and R.Ch. would like to express their thanks to the Scientific Grant Agency of the Ministry of
367 Education, Science, Research and Sport of the Slovak Republic (VEGA 1/0220/21).

369 References

- 370 [1] A.P. Abbott, D. Boothby, G. Capper, D.L. Davies, R.K. Rasheed, Deep Eutectic Solvents formed
371 between choline chloride and carboxylic acids: Versatile alternatives to ionic liquids, *J. Am.*
372 *Chem. Soc.* 126 (2004) 9142–9147. <https://doi.org/10.1021/ja048266j>.
- 373 [2] D. Deng, G. Han, Y. Jiang, Investigation of a deep eutectic solvent formed by levulinic acid with
374 quaternary ammonium salt as an efficient SO_2 absorbent, *New J. Chem.* 39 (2015) 8158–8164.
375 <https://doi.org/10.1039/c5nj01629k>.
- 376 [3] G. Li, Y. Jiang, X. Liu, D. Deng, New levulinic acid-based deep eutectic solvents: Synthesis and
377 physicochemical property determination, *J. Mol. Liq.* 222 (2016) 201–207.
378 <https://doi.org/10.1016/j.molliq.2016.07.039>.

- 379 [4] H. Wu, M. Shen, X. Chen, G. Yu, A.A. Abdeltawab, S.M. Yakout, New absorbents for hydrogen
380 sulfide: Deep eutectic solvents of tetrabutylammonium bromide/carboxylic acids and choline
381 chloride/carboxylic acids, *Sep. Purif. Technol.* 224 (2019) 281–289.
382 <https://doi.org/10.1016/J.SEPPUR.2019.04.082>.
- 383 [5] H.F. Hizaddin, M. Sarwono, M. Ali Hashim, I.M. Alnashef, M.K. Hadj-Kali, Coupling the
384 capabilities of different complexing agents into deep eutectic solvents to enhance the
385 separation of aromatics from aliphatics, *J. Chem. Thermodyn.* 84 (2015) 67–75.
386 <https://doi.org/10.1016/j.jct.2014.12.024>.
- 387 [6] N. Li, Y. Wang, K. Xu, Q. Wen, X. Ding, H. Zhang, Q. Yang, High-performance of deep eutectic
388 solvent based aqueous bi-phasic systems for the extraction of DNA, *RSC Adv.* 6 (2016) 84406–
389 84414. <https://doi.org/10.1039/c6ra17689e>.
- 390 [7] R. Yusof, E. Abdulmalek, K. Sirat, M.B.A. Rahman, Tetrabutylammonium bromide (TBABr)-
391 Based deep eutectic solvents (DESs) and their physical properties, *Molecules.* 19 (2014) 8011–
392 8026. <https://doi.org/10.3390/molecules19068011>.
- 393 [8] M.K. Alomar, M. Hayyan, M.A. Alsaadi, S. Akib, A. Hayyan, M.A. Hashim, Glycerol-based deep
394 eutectic solvents: Physical properties, *J. Mol. Liq.* 215 (2016) 98–103.
395 <https://doi.org/10.1016/j.molliq.2015.11.032>.
- 396 [9] F. Gabriele, M. Chiarini, R. Germani, M. Tiecco, N. Spreti, Effect of water addition on choline
397 chloride/glycol deep eutectic solvents: Characterization of their structural and
398 physicochemical properties, *J. Mol. Liq.* 291 (2019) 111301.
399 <https://doi.org/10.1016/j.molliq.2019.111301>.
- 400 [10] P. Makoś, G. Boczkaj, Deep eutectic solvents based highly efficient extractive desulfurization
401 of fuels – Eco-friendly approach, *J. Mol. Liq.* 296 (2019) 111916–111927.
402 <https://doi.org/10.1016/j.molliq.2019.111916>.
- 403 [11] R. Chromá, M. Vilková, I. Shepa, P. Makoś-Chełstowska, V. Andruch, Investigation of
404 tetrabutylammonium bromide-glycerol-based deep eutectic solvents and their mixtures with
405 water by spectroscopic techniques, *J. Mol. Liq.* 330 (2021) 115617.
406 <https://doi.org/10.1016/j.molliq.2021.115617>.
- 407 [12] T. Aissaoui, Y. Benguerba, M.K. AlOmar, I.M. AlNashef, Computational investigation of the
408 microstructural characteristics and physical properties of glycerol-based deep eutectic
409 solvents, *J. Mol. Model.* 23 (2017). <https://doi.org/10.1007/s00894-017-3450-5>.
- 410 [13] M. Mohan, P.K. Naik, T. Banerjee, V. V. Goud, S. Paul, Solubility of glucose in
411 tetrabutylammonium bromide based deep eutectic solvents: Experimental and molecular
412 dynamic simulations, *Fluid Phase Equilib.* 448 (2017) 168–177.
413 <https://doi.org/10.1016/j.fluid.2017.05.024>.
- 414 [14] P.K. Naik, S. Paul, T. Banerjee, Physicochemical Properties and Molecular Dynamics Simulations
415 of Phosphonium and Ammonium Based Deep Eutectic Solvents, *J. Solution Chem.* 48 (2019)
416 1046–1065. <https://doi.org/10.1007/s10953-019-00903-0>.
- 417 [15] M. Saha, M. Saha, M.S. Rahman, M.N. Hossain, D.E. Raynie, M.A. Halim, Molecular and
418 Spectroscopic Insights of a Choline Chloride Based Therapeutic Deep Eutectic Solvent, *J. Phys.
419 Chem. A.* 124 (2020) 4690–4699. <https://doi.org/10.1021/acs.jpca.0c00851>.
- 420 [16] E. Słupek, P. Makoś, Absorptive Desulfurization of Model Biogas Stream Using Choline
421 Chloride-Based Deep Eutectic Solvents, *Sustainability.* 12 (2020) 1619–1635.

- 422 <https://doi.org/10.3390/su12041619>.
- 423 [17] P. Makoś, E. Słupek, J. Gębicki, Extractive detoxification of feedstocks for the production of
424 biofuels using new hydrophobic deep eutectic solvents – Experimental and theoretical
425 studies, *J. Mol. Liq.* (2020) in press. <https://doi.org/10.1016/j.molliq.2020.113101>.
- 426 [18] P. Makoś, A. Przyjazny, G. Boczkaj, Hydrophobic deep eutectic solvents as “green” extraction
427 media for polycyclic aromatic hydrocarbons in aqueous samples, *J. Chromatogr. A.* 1570
428 (2018). <https://doi.org/10.1016/j.chroma.2018.07.070>.
- 429 [19] S. Kaur, A. Gupta, H.K. Kashyap, H.K. Kashyap, How Hydration Affects the Microscopic
430 Structural Morphology in a Deep Eutectic Solvent, *J. Phys. Chem. B.* 124 (2020) 2230–2237.
431 <https://doi.org/10.1021/acs.jpcc.9b11753>.
- 432 [20] M.E. Di Pietro, O. Hammond, A. Van Den Bruinhorst, A. Mannu, A. Padua, A. Mele, M. Costa
433 Gomes, Connecting chloride solvation with hydration in deep eutectic systems, *Phys. Chem.*
434 *Chem. Phys.* 23 (2021) 107–111. <https://doi.org/10.1039/d0cp05843b>.
- 435 [21] S. Zhu, H. Li, W. Zhu, W. Jiang, C. Wang, P. Wu, Q. Zhang, H. Li, Vibrational analysis and
436 formation mechanism of typical deep eutectic solvents: An experimental and theoretical
437 study, *J. Mol. Graph. Model.* 68 (2016) 158–175.
438 <https://doi.org/https://doi.org/10.1016/j.jmgm.2016.05.003>.
- 439 [22] V. Krishnakumar, V. Balachandran, T. Chithambarathanu, Density functional theory study of
440 the FT-IR spectra of phthalimide and N-bromophthalimide, *Spectrochim. Acta - Part A Mol.*
441 *Biomol. Spectrosc.* 62 (2005) 918–925. <https://doi.org/10.1016/j.saa.2005.02.051>.
- 442 [23] S. Simon, M. Duran, J.J. Dannenberg, How does basis set superposition error change the
443 potential surfaces for hydrogen-bonded dimers?, *J. Chem. Phys.* 105 (1996) 11024–11031.
444 <https://doi.org/10.1063/1.472902>.
- 445 [24] T. Lu, F. Chen, Multiwfn: A multifunctional wavefunction analyzer, *J. Comput. Chem.* 33 (2012)
446 580–592. <https://doi.org/10.1002/jcc.22885>.
- 447 [25] T. Lu, F. Chen, Quantitative analysis of molecular surface based on improved Marching
448 Tetrahedra algorithm, *J. Mol. Graph. Model.* 38 (2012) 314–323.
449 <https://doi.org/10.1016/j.jmgm.2012.07.004>.
- 450 [26] E.R. Johnson, S. Keinan, P. Mori-Sánchez, J. Contreras-García, A.J. Cohen, W. Yang, Revealing
451 noncovalent interactions, *J. Am. Chem. Soc.* 132 (2010) 6498–6506.
452 <https://doi.org/10.1021/ja100936w>.
- 453 [27] J.M. Martínez, L. Martínez, Packing optimization for automated generation of complex
454 system’s initial configurations for molecular dynamics and docking, *J. Comput. Chem.* 24
455 (2003) 819–825. <https://doi.org/10.1002/jcc.10216>.
- 456 [28] M. Parrinello, A. Rahman, Polymorphic transitions in single crystals: A new molecular
457 dynamics method, *J. Appl. Phys.* 52 (1981) 7182–7190. <https://doi.org/10.1063/1.328693>.
- 458 [29] S. Nosé, A unified formulation of the constant temperature molecular dynamics methods, *J.*
459 *Chem. Phys.* 81 (1984) 511–519. <https://doi.org/10.1063/1.447334>.
- 460 [30] S. Nosé, S. Nosé, Molecular Physics: An International Journal at the Interface Between
461 Chemistry and Physics A molecular dynamics method for simulations in the canonical
462 ensemble A molecular dynamics method for simulations in the canonical ensemble, *An Int. J.*

- 463 Interface Between Chem. Phys. Mol. Phys. 52 (1984) 255–268.
- 464 [31] H.J.C. Berendsen, J.R. Grigera, T.P. Straatsma, The missing term in effective pair potentials, J.
465 Phys. Chem. 91 (1987) 6269–6271. <https://doi.org/10.1021/j100308a038>.
- 466 [32] B. Hess, C. Kutzner, D. Van Der Spoel, E. Lindahl, GRGMACS 4: Algorithms for highly efficient,
467 load-balanced, and scalable molecular simulation, J. Chem. Theory Comput. 4 (2008) 435–447.
468 <https://doi.org/10.1021/ct700301q>.
- 469 [33] D. Van Der Spoel, E. Lindahl, B. Hess, G. Groenhof, A.E. Mark, H.J.C. Berendsen, GROMACS:
470 Fast, flexible, and free, J. Comput. Chem. 26 (2005) 1701–1718.
471 <https://doi.org/10.1002/jcc.20291>.
- 472 [34] H. Sasaki, S. Daicho, Y. Yamada, Y. Nibu, Comparable strength of OH-O versus OH- π hydrogen
473 bonds in hydrogen-bonded 2,3-benzofuran clusters with water and methanol, J. Phys. Chem.
474 A. 117 (2013) 3183–3189. <https://doi.org/10.1021/jp400676x>.
- 475 [35] P. Kumari, Shobhna, S. Kaur, H.K. Kashyap, Influence of Hydration on the Structure of Reline
476 Deep Eutectic Solvent: A Molecular Dynamics Study, ACS Omega. 3 (2018) 15246–15255.
477 <https://doi.org/10.1021/acsomega.8b02447>.
- 478